

A Paper/Polymer Hybrid Microfluidic Nanosensing Rotary Chip: From Efficient Reagent Delivery to Multiplexed Detection of Toxins

Maowei Dou and XiuJun Li*

Cite This: *Anal. Chem.* 2025, 97, 14830–14837

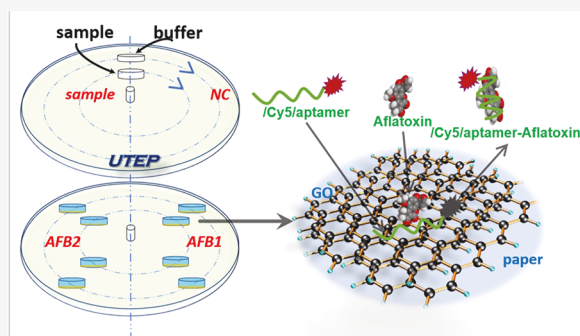
Read Online

ACCESS |

Metrics & More

Article Recommendations

ABSTRACT: In this study, we present a novel paper/polymer hybrid microfluidic Rotary Chip, integrated with aptamer-functionalized graphene oxide (GO) nanosensors, which enables not only efficient reagent delivery but also quantitative multiplexed detection. Rapid simultaneous detection of two major aflatoxins, aflatoxin B1 (AFB1) and aflatoxin B2 (AFB2), was successfully achieved to demonstrate the effectiveness of this hybrid rotary chip. Aflatoxins, as potent natural carcinogens, represent a significant global food safety challenge. Rapid and sensitive detection methods are crucial for effective monitoring. The RotaryChip design involves manually rotating the top poly(methyl methacrylate) (PMMA) plate over the bottom plate around a central screw, providing a simple strategy for rapid and efficient reagent delivery for multiplexed assays and high-throughput analysis without the need for sophisticated external pumps or pneumatic valves. The paper substrate in this hybrid microfluidic plate facilitates the facile integration of nanosensors in detection wells without the need for elaborate surface modification. The entire assay was completed in approximately 30 min and did not involve any washing steps. The platform achieved detection limits as low as 0.7 $\mu\text{g}/\text{kg}$ for AFB1 and 0.5 $\mu\text{g}/\text{kg}$ for AFB2. We further validated the platform by accurately detecting and quantifying AFB1 and AFB2 in spiked cooking oil samples with high specificity. Owing to its high simplicity and specificity, fast analysis, simple and efficient reagent delivery, and its multiplexing and quantitative capability, this paper/PMMA hybrid microfluidic nanosensing platform has tremendous potential for environmental and food safety surveillance, including multiplexed detection of different toxins and pathogens, particularly in low-resource settings.



INTRODUCTION

Aflatoxins are toxic secondary metabolites primarily produced by *Aspergillus flavus* and *Aspergillus parasiticus*. These compounds are some of the most potent naturally occurring carcinogens and are commonly detected in agricultural products and food items such as corn, peanuts, cottonseed, various nuts, almonds, figs, pistachios, spices, as well as dairy products like milk and cheese.¹ Of the various aflatoxin types, aflatoxin B1 (AFB1) is considered the most toxic and carcinogenic, with the International Agency for Research on Cancer (IARC) classifying it as a group I human carcinogen (LD50 = 6.5–16.5 mg/kg). Aflatoxin B2 (AFB2) is also classified as a group I human carcinogen, though it is less toxic than AFB1.^{2,3} Regulatory agencies have established stringent limits for aflatoxin contamination to mitigate the risk of exposure. The United States has set a maximum permitted level of 20 $\mu\text{g}/\text{kg}$ for total aflatoxins,⁴ while the European Union (EU) enforces even stricter limits of 2 $\mu\text{g}/\text{kg}$ for AFB1 and 4 $\mu\text{g}/\text{kg}$ for total aflatoxins in food products.⁵

Aflatoxin contamination remains a global food safety issue, with an estimated 4.5 billion people, especially in low-income areas of Southeast Asia and Sub-Saharan Africa, chronically

exposed to aflatoxin-contaminated food.⁶ Chronic dietary exposure to aflatoxins has been identified as a major risk factor for hepatotoxicity and hepatocellular carcinoma (HCC),^{6–8} which accounts for over 600,000 deaths annually, with the majority of cases concentrated in regions with heavy aflatoxin exposure.^{9,10} Aflatoxin exposure varies globally, with higher levels in regions consuming maize and peanuts, such as sub-Saharan Africa and Southeast Asia, while stricter regulations in the EU and North America reduce exposure. Chronic ingestion poses serious health risks, including liver cancer and immune suppression. This highlights the need for rapid and sensitive detection methods for multiple aflatoxins for food safety monitoring due to frequent cocontaminations,¹¹ especially in low-resource settings.

Received: May 20, 2025

Revised: June 19, 2025

Accepted: June 20, 2025

Published: June 27, 2025



Traditional methods for detecting aflatoxins include chromatographic techniques such as high-performance liquid chromatography (HPLC),^{12,13} liquid chromatography–mass spectrometry (LC–MS),^{14–16} and immunoassays like enzyme-linked immunosorbent assay (ELISA).^{17,18} While chromatographic methods offer high sensitivity, they require expensive, complex instrumentation and complicated time-consuming procedures. ELISA,¹⁹ though widely used, involves lengthy incubation times and multiple washing steps, limiting its practicality for rapid screening.^{19–21}

Aptamers, which are single-stranded DNA or RNA (ssDNA or ssRNA) molecules, offer a promising alternative to antibodies in analytical assays due to their high specificity and affinity for various targets, including small molecules, proteins, and even whole cells.^{22–25} Also, graphene oxide (GO) is known for its strong fluorescence quenching ability, biocompatibility, and high surface area, making it an ideal nanomaterial for biosensing applications. Recently, aptamer-GO-based methods have been developed for the detection of AFB1, but most of them need complex synthesis or conjugation procedures and only detect a single aflatoxin.^{26–33,25,34,35} For instance, Lu et al. reported an aptamer-based assay using quantum dots (Q-dots) and GO for AFB1 detection.²⁸ However, the complex synthesis and conjugation processes involved in these assays, which can take over 12 h, as well as the focus on single aflatoxin detection, limit their application for rapid multiplexed analysis. There is a need to develop simple, cost-effective, and integrated methods for rapid, sensitive, and quantitative multiplexed detection of aflatoxins AFB1 and AFB2.

Microfluidic platforms provide an ideal solution for multiplexed biological analyses due to their low reagent consumption, rapid processing, and potential for integration and miniaturization.^{36–44} Their advantage of high portability also enables microfluidic devices to be an excellent candidate for point-of-care detection.^{37,45–51} For instance, we developed different cost-effective microfluidic systems combined with aptamers-functionalized GO nanosensors for rapid detection of pathogens and estradiol in low-resource settings.^{42,52,53} Additionally, different groups have developed various microfluidic devices for multiplexed assays.^{54–57} However, these approaches often rely on sophisticated mechanisms, such as external pumps or pneumatic valves, to control reagent flow and distribution across multiple reaction microwells,⁵⁸ making them impractical for point-of-care multiplexed analysis. Ismagilov's group developed a simple SlipChip format microfluidic device for simpler reagent delivery and multiplexing.⁵⁴ However, during the slipping movement, it is difficult to slide the top plate over the bottom plate in a straight path without directional deviations, as the lack of a connection between the two plates allows the trajectory to easily veer off course. If the trajectory veers off the course, it may result in inconsistent reagent delivery, or deliver different volumes of the reagents to parallel microwells, and thus negatively impact the accuracy of different parallel analyses in a multiplexed assay, because the quantity of reagents often affects the assay results.

In this work we have developed a new paper/polymer hybrid microfluidic rotary chip (i.e., RotaryChip) incorporating aptamer-functionalized GO nanosensors, which enables not only efficient reagent delivery but also quantitative multiplexed detection. This RotaryChip has been employed for the simple, rapid, multiplexed, and quantitative detection of aflatoxins

AFB1 and AFB2. Two poly(methyl methacrylate) (PMMA) plates were tightened by a central screw to form a closed microsystem to minimize evaporation during incubation. The central screw also functions as a spindle, enabling the manual rotation of the top PMMA layer over the other around the central screw. As all inlet reservoirs rotate around the central screw, the inlet reservoir trajectory on the top plate will not veer off course, providing enhanced alignment and precise reagent delivery, without the need for sophisticated external pumps or pneumatic valves. Our paper/PMMA platform also takes advantage of both chip substrates.^{37,59} For example, the introduction of paper to this hybrid device facilitates simple nanosensor immobilization, without complicated surface modification. This microfluidic nanosensing RotaryChip further employs a simple one-step “turn-on” detection strategy even without washing steps, wherein aptamers labeled with fluorophores are released from the GO surface upon binding to target molecules, restoring the fluorescence signal. All these features of the hybrid RotaryChip allows for simple, simultaneous, sensitive, quantitative, and specific detection of both toxins in a single assay format, with LODs as low as 0.7 and 0.5 $\mu\text{g}/\text{kg}$ for AFB1 and AFB2, respectively, well below the threshold set by various regulatory agencies. Successful detection of AFB1 and AFB2 was further validated by using spiked real samples. Compared to ELISA and HPLC/LC–MS, our RotaryChip platform offers significant advantages in cost, simplicity, and field applicability. Unlike HPLC/LC–MS, which requires expensive instrumentation, trained personnel, and extensive sample preparation, our method is cost-effective and can be performed without sophisticated equipment. Compared to ELISA, our approach eliminates the need for multiple washing and incubation steps, reducing assay time and complexity. The RotaryChip's passive fluid delivery system further enhances ease of use, making it more suitable for rapid on-site testing in resource-limited settings. This study provides a simple microfluidic nanosensing strategy for multiplexed quantitative detection of multiple aflatoxins and other biochemicals, demonstrating a simple, low-cost, rapid, portable, and effective tool for food safety surveillance at the point of need.

■ EXPERIMENTAL SECTION

Chemicals and Materials. Poly(methyl methacrylate) (PMMA) sheets were purchased from McMaster-Carr (Los Angeles, CA), and Whatman#1 chromatography paper was obtained from Sigma-Aldrich (St. Louis, MO). GO was purchased from Graphene Laboratories (Calverton, NY). AFB1, AFB2, and all other chemicals were also obtained from Sigma-Aldrich and used without further purification. All solutions were prepared with ultrapure Milli-Q water (18.2 M Ω cm) from a Millipore Milli-Q system (Bedford, MA), unless otherwise stated.

DMSO was used as a solvent to dissolve AFB1 and AFB2 due to their limited solubility in aqueous solutions, allowing effective initial dispersion before dilution. The hybridization buffer, composed of 0.1370 M NaCl, 0.0027 M KCl, 0.0100 M Na₂HPO₄, 0.0018 M KH₂PO₄, 0.075 M sodium citrate, and 0.1% sodium dodecyl sulfate (SDS), was used to maintain reagent stability and promote efficient interactions during the assay. To prepare the aflatoxin standard solutions, AFB1 and AFB2 were first dissolved in DMSO and then diluted with hybridization buffer at a ratio of 1:9 (v/v) for the assays. For the spiked cooking oil samples, aflatoxins were first dissolved in

Table 1. Sequences of Aptamers Used for Detection of AFB1 and AFB2

aptamer	sequences (5'–3')	length (mer)
AFB1	/Cy5/GTTGGGCACGTGTTGTCTCTCTGTGTCTCGTGCCCTTCGCTAGGCCCA	50
AFB2	/Cy5/AGCAGCACAGAGGTCAGATGCTGACACCCTGGACCTGGGATTCCGGAAGTTTCCGGTACCTATGCGTGCTACCGTGAA	80

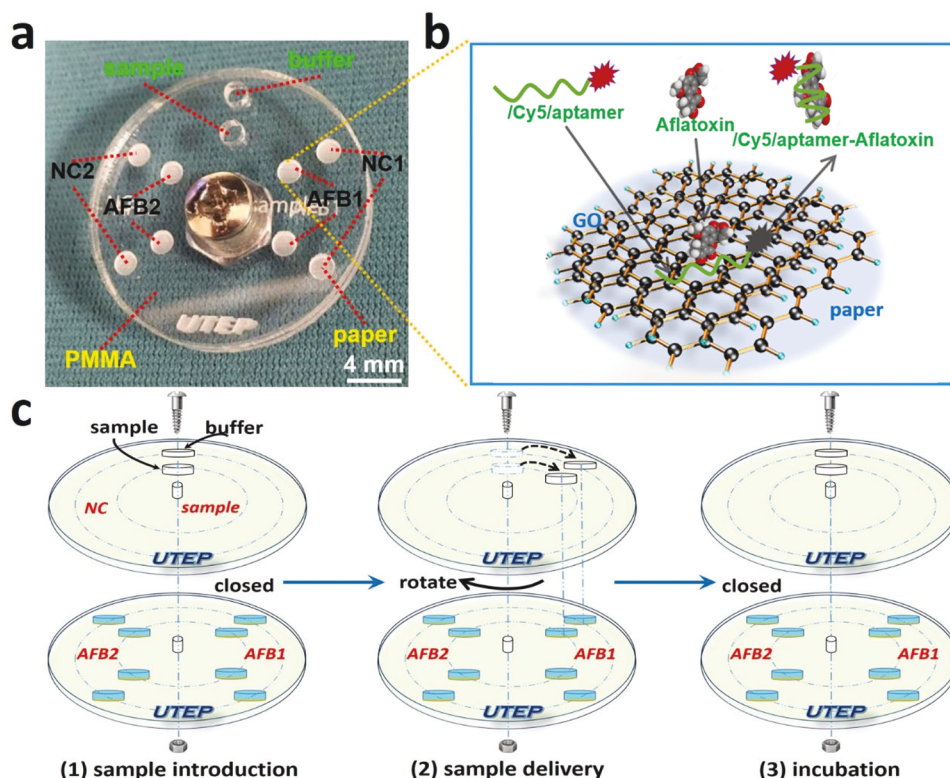


Figure 1. Design and schematic of the paper/PMMA hybrid microfluidic RotaryChip for multiplexed detection of aflatoxins. (a) Photograph of the microfluidic RotaryChip; (b) close-up of the detection well, illustrating the principle of the aptamer-functionalized GO nanosensors-based assay for aflatoxins. (c) Schematic of the process for sample introduction, delivery, and incubation for multiplexed aflatoxin detection on the RotaryChip.

DMSO and then serially diluted with corn oil to the desired concentrations. The solution was sonicated for 10 min to ensure uniform dispersion of aflatoxins. Following sonication, the samples were vortexed and stored at 4 °C until analysis. The mixture was subsequently diluted with hybridization buffer at a 1:9 ratio (v/v) to create a compatible environment for efficient detection.

The sequences of the aptamers used for AFB1²⁶ and AFB2⁶⁰ detection are listed in Table 1. The aptamers were fluorescently labeled with Cy5 at the 5' end and were synthesized by Integrated DNA Technologies (Coralville, IA).

Design and Fabrication of the Paper/Polymer Hybrid Microfluidic RotaryChip. The rotary hybrid microfluidic platform consisted of two PMMA layers fastened with a screw, each with a diameter of 2.5 cm and a depth of 1.2 mm. As illustrated in Figure 1, the top PMMA plate contained two 2 mm-diameter holes, designated for sample and blank buffer delivery. The bottom PMMA plate featured six detection wells, each with a diameter of 2 mm and a depth of 0.7 mm. These wells were allocated for the detection of AFB1 and AFB2, and their respective negative controls (NC1 and NC2). The sample delivery hole in the top plate was aligned with the inner wells (for AFB1 and AFB2), while the blank buffer delivery hole was aligned with the outer wells (for NC1 and NC2).

A paper disk (2 mm in diameter) was placed inside each detection well, forming a paper/PMMA hybrid microfluidic

device. Subsequently, 0.7 μL of a GO solution (0.02 mg/mL in water) and 0.7 μL of an aptamer solution (1 nM in hybridization buffer) were added to the wells and absorbed by the paper via the capillary action. The detection wells for AFB1 and AFB2 were thus preloaded with aptamer-functionalized GO nanosensors, and the negative control wells (NC1 and NC2) were preloaded with the same respective nanosensors for AFB1 and AFB2. Thus, the paper/polymer hybrid microfluidic RotaryChip became ready for use. The detection wells and paper disks were directly cut using an Epilog Zing 16 laser cutter (Golden, CO), which enabled rapid and precise fabrication.

Assay Procedures. The following protocol was used for multiplexed detection of aflatoxins using the microfluidic rotary chip. (1) Sample loading: 6 μL of the sample solution and 6 μL of hybridization buffer were introduced into the sample deliver hole and blank buffer delivery hole, respectively, on the top plate (Figure 1c-1). (2) Sample distribution: The top plate was manually rotated to align the sample and buffer delivery holes with the corresponding detection wells and the negative control wells on the bottom plate (Figure 1c-2), allowing the samples and buffer to distribute evenly across the wells. (3) Incubation: After sample distribution, the top plate was rotated back to its original position, covering and sealing the detection wells (Figure 1c-3). The plate was incubated in a humid, dark chamber at 40 °C for 20 min. (4) Fluorescence

measurement: After incubation, the device was scanned using a Nikon fluorescence microscope (Melville, NY) or a portable fluorescence imager equipped with Cy5 excitation and emission filters to measure the fluorescence intensity in each well, reflecting the presence of AFB1 and AFB2 based on aptamer displacement from the GO surface. This method allows for simultaneous quantification of AFB1 and AFB2 in both standard solutions and spiked cooking oil samples, providing a rapid, sensitive, and efficient multiplexed approach for aflatoxin analysis.

RESULTS AND DISCUSSION

Principle of the Hybrid Microfluidic RotaryChip for Multiplexed Detection of Aflatoxins. The fabrication of the paper/PMMA hybrid microfluidic device (Figure 1a) is both straightforward and rapid, taking only a few minutes. The low-cost paper disks placed in the detection wells (Figure 1a,b) serve as a porous substrate that simplifies the integration of ssDNA aptamer-functionalized GO nanosensors without requiring complex surface treatment. The large effective surface area of the porous paper enhances reaction kinetics, making it ideal for rapid assays.⁶¹ Our previous studies demonstrate that the high surface-to-volume ratio of the paper substrate facilitates the uniform distribution of ssDNA and ensures stable long-term assay performance.⁶² Unlike single paper substrate-based devices,^{63,64} the hybrid paper/PMMA microfluidic system draws more benefits from both device substrates.^{19,37,39,65} While paper facilitates simple nanosensor immobilization, PMMA plates enable efficient reagent delivery, and create a closed environment, minimizing evaporation losses. Thus, this hybrid device maximizes the benefits of paper-based substrates while overcoming their inherent limitations.

While graphene oxide (GO) has been widely utilized in biosensing applications,⁶⁶ the novelty of our approach lies in the integration of GO within a passive fluid-driven rotary chip. Unlike conventional microfluidic systems that rely on microchannels or external pumps for fluid transport, our platform employs a passive fluid delivery mechanism driven by rotational actuation. This design eliminates the need for complex fluid control systems, making the assay more user-friendly and suitable for low-resource settings. Additionally, unlike SlipChip, which requires lateral sliding with precise alignment, our design ensures reagent distribution through controlled rotation, minimizing manual errors. While the device does not incorporate conventional microfluidic channels, the term “microfluidic” here refers to the precise manipulation and control of microliter-scale fluid volumes within a confined architecture, justifying the scope of this work in microfluidics. The combination of GO nanosensors with this novel reagent delivery approach enhances detection efficiency while maintaining a cost-effective and portable format, setting our work apart from existing GO-based biosensors.

As illustrated in Figure 1b, the assay principle relies on GO's fluorescence quenching properties, which are distance-dependent. Initially, the fluorescence of Cy5-labeled aptamers is quenched by GO.⁶⁷ When the target aflatoxins are introduced, the aptamers bind specifically to the targets, causing a conformation change in the DNA from a random coil to a folded structure. This reduces the affinity between the aptamer and GO, releasing the aptamer from the GO surface and restoring its fluorescence, enabling aflatoxin detection.

The microfluidic RotaryChip was designed for rapid and efficient sample introduction and reagent delivery to many microwells. The two PMMA plates are fastened with a screw rather than being permanently bonded (Figure 1a,c), allowing the plate to be opened for easy assembly and replacement of paper disks. To minimize potential contamination, the device is intended for single-use, ensuring reliable and consistent results while reducing the risk of cross-contamination. The central screw also functions as a spindle, enabling the manual rotation of one PMMA layer over the other. As shown in Figure 1c, some sample introduction reservoirs are fabricated on the top PMMA plate (one inner inlet reservoir for sample introduction and the other inlet reservoir for buffer introduction as control), while multiple microwells are designed at the bottom PMMA plate exactly underneath the rotary circular trajectory of the two introduction reservoirs on the top PMMA plate. After the sample and the buffer reservoirs are loaded with their corresponding reagents, we can manually rotate the top PMMA plate around the center screw. When the inlet reservoirs just pass above these different microwells (i.e., AFB1 and NC1 microwells first, respectively) on the bottom PMMA plate, reagents will be in touch with paper disks in microwells underneath, and thus samples and reagent are introduced from inlet reservoirs above into these wells on the bottom PMMA plate efficiently via the capillary action and gravity, without the need for external pumps or pneumatic valves. These features are particularly advantageous for low-resource settings where multiplexed assays are required.

After completing reagent delivery to AFBN1 microwells, when we continue to rotate the top PMMA plate, reagents will subsequently and automatically be delivered to AFB2 and NC2 microwells separately. If we rotate the top PMMA plate to other locations where the inlet reservoirs are not aligned with microwells on the bottom plate, this will put the rotary hybrid microfluidic device into a “Closed” status, allowing long-term incubation without significant reagent loss. Please note that in this work, we only designed 4 microwells to illustrate the principle of the paper/PMMA hybrid microfluidic RotaryChip for rapid reagent delivery. However, the number of microwells to receive reagents can be scaled up to deliver reagents to tens of microwells rapidly, upon demand. Similarly, the number of inlet reservoirs can also be increased to allow the simultaneous delivery of many different kinds of reagents simultaneously.

Multiplexed Assays on the Hybrid RotaryChip for AFB1 and AFB2. To evaluate the performance of the microfluidic platform for multiplexed detection, standard solutions containing 100 $\mu\text{g}/\text{kg}$ AFB1 and AFB2 were tested. As shown in Figure 2, fluorescence images and corresponding intensity measurements demonstrated the successful detection of both aflatoxins. Before sample introduction, the detection wells displayed minimal fluorescence (Figure 2a), indicating effective quenching of the Cy5-labeled aptamers by GO. After incubation, strong fluorescence signals were observed in the wells designated for AFB1 and AFB2, while the negative control wells showed minimal fluorescence (Figure 2b). The fluorescence recoveries in the AFB1 and AFB2 wells were approximately eight folds higher than in the negative control wells (Figure 2c), confirming the device's ability to distinguish between the target analytes and controls. The well-defined fluorescence recovery and target-specific nanosensors form the basis for accurate, and quantitative multiplexed assays.

Compared with open paper-based microsystems,^{68,69} the reagent volume used in the RotaryChip is minimal, which

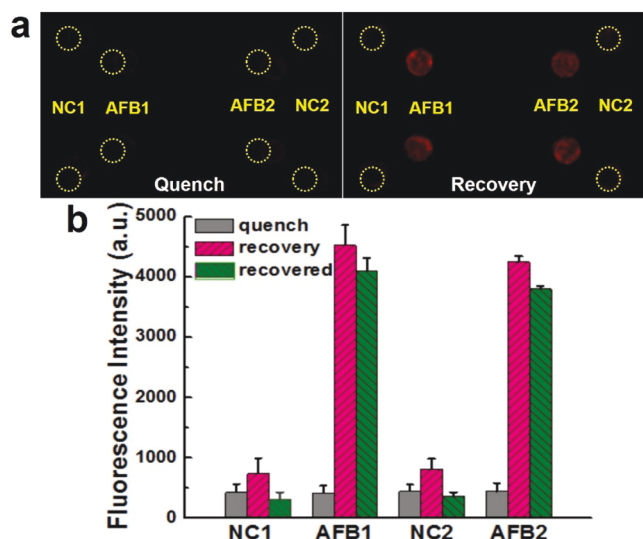


Figure 2. Multiplexed detection of AFB1 and AFB2 on the RotaryChip. (a) Fluorescence images of detection wells before and after the recovery of fluorescence. (b) Corresponding fluorescence intensities, with standard solutions containing 100 $\mu\text{g}/\text{kg}$ each of AFB1 and AFB2. Error bars represent the standard deviations ($n = 4$).

optimizes cost-efficiency and reduces waste. While evaporation could be a concern in prolonged assays, the rapid detection process in our platform minimizes its impact, ensuring reliable and consistent results within the intended operational time frame; and the closed system further minimizes evaporation during incubation. The entire aptamer-functionalized GO nanosensing process can be completed within 30 min, eliminating the need for time-consuming washing steps common in conventional antibody-based assays.^{17,40}

Specificity Test. The specificity of the approach was evaluated using separate tests for AFB1 and AFB2, which have the most similar chemical structures among mycotoxins. Specific aptamer-functionalized GO nanosensors for AFB1

and AFB2 were employed, and standard solutions of 100 $\mu\text{g}/\text{kg}$ AFB1 and 100 $\mu\text{g}/\text{kg}$ AFB2 were introduced separately.

As shown in Figure 3, only the target aflatoxins generated strong fluorescence recovery with their corresponding aptasensors, while nontarget interactions resulted in significantly lower fluorescence. The fluorescence recovery for the specific aptasensors was approximately 4-fold higher than that from the noncorresponding aptasensors and about 8-fold higher than negative controls. The results that structurally similar mycotoxins like AFB1 and AFB2 were able to be identified indicated the high specificity of our approach.

Quantitative Detection. The detection sensitivity was further investigated by testing serial 10-fold dilutions of aflatoxin standard solutions. As shown in Figures 4 and 5,

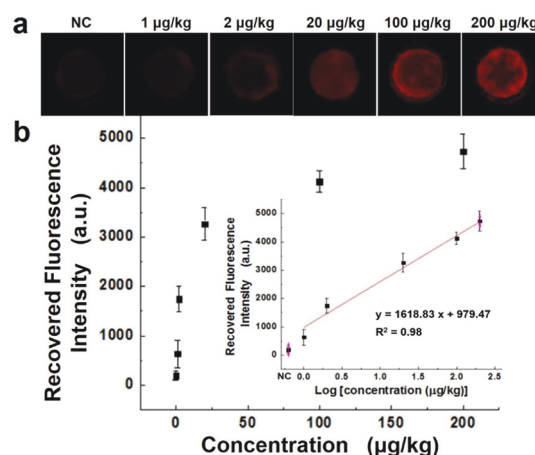


Figure 4. Calibration curve for AFB1 detection. Recovered fluorescence intensity was plotted against the concentration of AFB1, showing a linear relationship with an R^2 value of 0.98. Error bars represent the standard deviations ($n = 4$).

the recovered fluorescence intensities were plotted against the logarithm of aflatoxin concentrations, resulting in linear calibration curves for both AFB1 and AFB2 in the range of

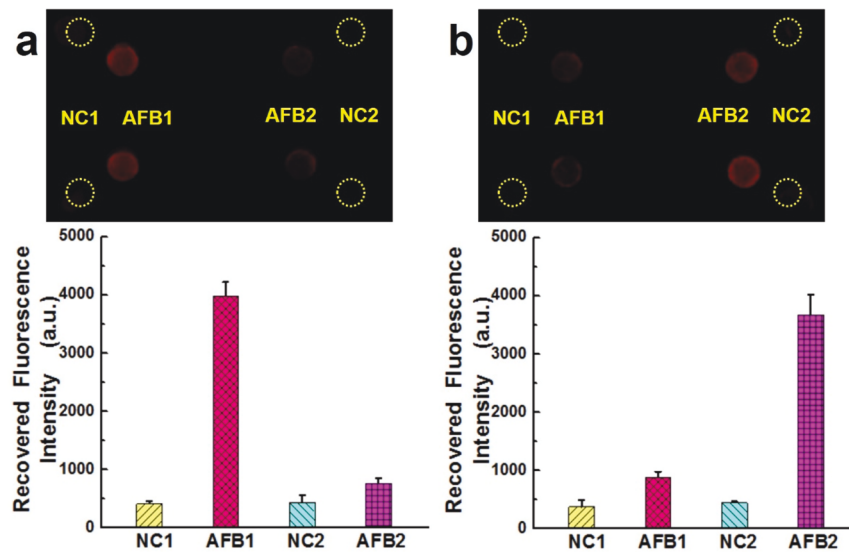


Figure 3. Fluorescence images and intensities for the specificity test of AFB1 (a) and AFB2 (b). AFB1 and 100 $\mu\text{g}/\text{kg}$ AFB2 standard solutions (100 $\mu\text{g}/\text{kg}$ each) were tested separately to assess the specificity of the aptamer-based nanosensors. Error bars represent the standard deviations ($n = 4$).

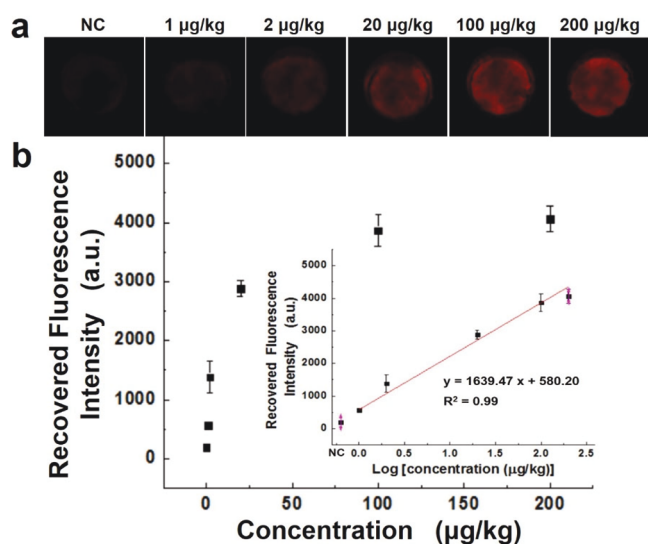


Figure 5. Calibration curve for AFB2 detection. Recovered fluorescence intensity was plotted against the concentration of AFB2, showing a linear relationship with an R^2 value of 0.99. Error bars represent the standard deviations ($n = 4$).

1.0–200.0 $\mu\text{g}/\text{kg}$, with R^2 values of 0.98 and 0.99, respectively. The limit of detection (LOD) values for AFB1 and AFB2 were determined using a signal-to-noise ratio (S/N) of 3, calculated as the lowest concentration where the signal exceeded three times the standard deviation of the blank. The resulting LODs were 0.7 $\mu\text{g}/\text{kg}$ for AFB1 and 0.5 $\mu\text{g}/\text{kg}$ for AFB2, confirming the method's high sensitivity, which are well below the most stringent regulatory limits.^{4,5} The detection sensitivity of the RotaryChip platform is comparable to or slightly higher than reported values from HPLC-based methods (typically in the range of 0.1–0.5 $\mu\text{g}/\text{kg}$). While HPLC remains the gold standard method for aflatoxin detection, our method offers a significant advantage in terms of simplicity, speed, and field applicability.

Real Sample Test. Cooking oils derived from crop plants, such as corn, have gained popularity as healthier alternatives to animal fats, but there are concerns about aflatoxin contamination in these oils.⁷⁰ Several studies have reported aflatoxin contamination in commercial edible oils, with some exceeding the U.S. FDA safety limits.^{11,71} To demonstrate the application of this RotaryChip for real-world samples, we tested cooking oils spiked with aflatoxins. In this work, we focused on spiked cooking oil samples due to their common use in food preparation. However, including a broader range of food matrices would strengthen our study and future studies will extend the application to other food matrices.

To minimize potential interference from unprocessed samples, the cooking oil samples were pretreated by dissolving aflatoxins in DMSO, followed by serial dilution in oil and further dilution in hybridization buffer. This step ensured compatibility with the assay and reduced matrix effects. Control experiments with blank oil samples demonstrated that background interference was negligible, confirming the robustness of the detection platform.

As shown in Table 2, the platform demonstrated accurate detection of two different concentrations of aflatoxin, with recovery rates ranging from 88.3 to 105.5%. These results confirmed the accuracy of the microfluidic platform for multiplexed aflatoxin detection in real-world food matrices.

Table 2. Results of Aflatoxin Detection in Spiked Cooking Oil Samples ($n = 4$)

aflatoxin	spiked ($\mu\text{g}/\text{kg}$)	measured ($\mu\text{g}/\text{kg}$)	recovery (%)	CV (%)
AFB1	2.0	2.1	105.5	14.9
	20.0	18.4	92.0	12.3
AFB2	6.0	5.3	88.3	7.0
	16.0	15.2	95.0	9.0

Although this study primarily investigated aflatoxin detection in spiked cooking oil samples, the RotaryChip platform can be extended to other liquid-based food matrices with suitable pretreatment.

CONCLUSIONS

In this study, we developed a novel paper/polymer hybrid microfluidic rotary chip integrated with aptamer-functionalized nanosensors for rapid, efficient reagent delivery and multiplexed detection. This has been successfully demonstrated through the simultaneous quantitative detection of two aflatoxins. The rotary chip design enables precise and controlled reagent distribution across multiple microwells without requiring external pumps, pneumatic valves, or robotic equipment, making it an ideal platform for multiplexed assays in low-resource settings.

The hybrid paper/polymer architecture leverages the strengths of both materials: paper facilitates simple nanosensor immobilization, while PMMA plates enhance reagent delivery efficiency and create a sealed environment. This integration maximizes the benefits of paper-based substrates while overcoming their inherent limitations.

The device achieved sensitive and simultaneous detection of AFB1 and AFB2, with LODs as low as 0.7 and 0.5 $\mu\text{g}/\text{kg}$, respectively, within approximately 30 min. This platform offers a straightforward nanosensing approach that eliminates the need for surface treatment or washing steps, streamlining detection for rapid deployment. Furthermore, its adaptability for detecting various toxic compounds or pathogens by simply modifying aptamers underscores its broad applicability in environmental and food safety surveillance and other multiplexed bioassays, particularly in resource-limited settings.

AUTHOR INFORMATION

Corresponding Author

XiuJun Li – Department of Chemistry and Biochemistry and Forensic Science, Border Medical Research Center, and Environmental Science and Engineering, University of Texas at El Paso, El Paso, Texas 79968, United States;
orcid.org/0000-0002-7954-0717; Email: xli4@utep.edu

Author

Maowei Dou – Department of Chemistry and Biochemistry, University of Texas at El Paso, El Paso, Texas 79968, United States

Complete contact information is available at:
<https://pubs.acs.org/10.1021/acs.analchem.5c03028>

Notes

The authors declare the following competing financial interest(s): The authors have submitted a patent application.

ACKNOWLEDGMENTS

We would like to acknowledge financial support from NIH/NIAID (R41AI162477), the U.S. NSF (IIP2122712 and CHE2216473), the Cancer Prevention and Research Institute of Texas (CPRIT; RP210165), the TTUHSC-UTEP Joint Seed Grant, and the AAFS Foundation Research Lucas grant. We are also grateful for the prior financial support to our research from the NIH/NIAID (R21AI107415), the NIH/NIGMS (SC2GM105584), the NIH/NIMHD RCMI Pilot grant (5G12MD007593-22), the NIH BUILDing Scholar Summer Sabbatical Award, the NSF (IIP1953841, IIP2052347, and DMR1827745), the DOT (CARTEEH), the Philadelphia Foundation, the Medical Center of the Americas Foundation (MCA), the University of Texas (UT) System for the STARS award, and the UTEP for IDR, URI, and MRAP awards.

REFERENCES

- (1) Abrar, M.; Anjum, F. M.; Butt, M. S.; Pasha, I.; Randhawa, M. A.; Saeed, F.; Waqas, K. *Critical reviews in food science and nutrition* **2013**, *53* (8), 862–874.
- (2) Meissonnier, G. M.; Pinton, P.; Laffitte, J.; Cossalter, A.-M.; Gong, Y. Y.; Wild, C. P.; Bertin, G.; Galtier, P.; Oswald, I. P. *Toxicology and applied pharmacology* **2008**, *231* (2), 142–149.
- (3) Nabok, A. V.; Mustafa, M. K.; Tsargorodskaya, A.; Starodub, N. F. *BioNanoScience* **2011**, *1* (1–2), 38–45.
- (4) Price, W. D.; Lovell, R. A.; McChesney, D. G. *J. Anim. Sci.* **1993**, *71* (9), 2556–2562.
- (5) Romagnoli, B.; Menna, V.; Gruppioni, N.; Bergamini, C. *Food Control* **2007**, *18* (6), 697–701.
- (6) Hamid, A. S.; Tesfamariam, I. G.; Zhang, Y.; Zhang, Z. G. *Oncology letters* **2013**, *5* (4), 1087–1092.
- (7) Dai Long, X.; Ma, Y.; Wei, Y. P.; Deng, Z. L. *Hepatol. Res.* **2006**, *36* (1), 48–55.
- (8) Wu, H.-C.; Wang, Q.; Yang, H.-I.; Ahsan, H.; Tsai, W.-Y.; Wang, L.-Y.; Chen, S.-Y.; Chen, C.-J.; Santella, R. M. *Cancer Epidemiology Biomarkers & Prevention* **2009**, *18* (3), 846–853.
- (9) Wild, C. P.; Gong, Y. Y. *Carcinogenesis* **2010**, *31* (1), 71–82.
- (10) Parkin, D. M. *International journal of cancer* **2006**, *118* (12), 3030–3044.
- (11) Junsai, T.; Poapolathep, S.; Sutjarit, S.; Giorgi, M.; Zhang, Z.; Logrieco, A. F.; Li, P.; Poapolathep, A. *Foods* **2021**, *10* (11), 2795.
- (12) Lai, X. W.; Sun, D. L.; Ruan, C. Q.; Zhang, H.; Liu, C. L. *J. Sep. Sci.* **2014**, *37* (1–2), 92–98.
- (13) Amirkhizi, B.; Arefhosseini, S. R.; Ansarin, M.; Nemati, M. *Food Addit. Contam.: Part B* **2015**, *8* (4), 245–249.
- (14) Rubert, J.; Fapohunda, S.; Soler, C.; Ezekiel, C.; Mañes, J.; Kayode, F. *Food Control* **2013**, *32* (2), 673–677.
- (15) Rubert, J.; Soler, C.; Mañes, J. *Food chemistry* **2012**, *133* (1), 176–183.
- (16) Abia, W. A.; Warth, B.; Sulyok, M.; Krska, R.; Tchana, A. N.; Njobeh, P. B.; Dutton, M. F.; Moundipa, P. F. *Food Control* **2013**, *31* (2), 438–453.
- (17) Rossi, C. N.; Takabayashi, C. R.; Ono, M. A.; Saito, G. H.; Itano, E. N.; Kawamura, O.; Hirooka, E. Y.; Ono, E. Y. S. *Food Chem.* **2012**, *132* (4), 2211–2216.
- (18) Mozaffari Nejad, A. S.; Sabouri Ghannad, M.; Kamkar, A. *Toxin Reviews* **2014**, *33* (4), 151–154.
- (19) Sanjay, S. T.; Li, M.; Zhou, W.; Li, X.; Li, X. *Microsystems & Nanoengineering* **2020**, *6* (1), 28.
- (20) Li, C.; Zhou, W.; Ruiz, A. G.; Mohammadi, Y.; Li, Q.; Zhang, S.; Li, X.; Fu, G. *TrAC Trends in Analytical Chemistry* **2024**, *177*, No. 117809.
- (21) Timilsina, S. S.; Li, X. *Lab Chip* **2024**, *24* (21), 4962–4973.
- (22) Lv, M.; Zhou, W.; Tavakoli, H.; Bautista, C.; Xia, J.; Wang, Z.; Li, X. *Biosens Bioelectron* **2021**, *176*, No. 112947.
- (23) Huang, K.-J.; Liu, Y.-J.; Zhang, J.-Z.; Cao, J.-T.; Liu, Y.-M. *Biosens. Bioelectron.* **2015**, *67*, 184–191.
- (24) Song, S.; Wang, L.; Li, J.; Fan, C.; Zhao, J. *TrAC Trends in Analytical Chemistry* **2008**, *27* (2), 108–117.
- (25) Ebanks, F.; Nasrallah, H.; Garant, T. M.; McConnell, E. M.; DeRosa, M. C. *Advanced Agrochem* **2023**, *2* (3), 221–230.
- (26) Shim, W.-B.; Kim, M. J.; Mun, H.; Kim, M.-G. *Biosens. Bioelectron.* **2014**, *62*, 288–294.
- (27) Seok, Y.; Byun, J.-Y.; Shim, W.-B.; Kim, M.-G. *Analytica chimica acta* **2015**, *886*, 182–187.
- (28) Lu, Z.; Chen, X.; Wang, Y.; Zheng, X.; Li, C. M. *Microchimica Acta* **2015**, *182* (3–4), 571–578.
- (29) Shim, W.-B.; Mun, H.; Joung, H.-A.; Ofori, J. A.; Chung, D.-H.; Kim, M.-G. *Food Control* **2014**, *36* (1), 30–35.
- (30) Castillo, G.; Spinella, K.; Poturnayová, A.; Šnejdárková, M.; Mosiello, L.; Hianik, T. *Food Control* **2015**, *52*, 9–18.
- (31) Guo, X.; Wen, F.; Zheng, N.; Luo, Q.; Wang, H.; Wang, H.; Li, S.; Wang, J. *Biosens. Bioelectron.* **2014**, *56*, 340–344.
- (32) Castillo, G.; Poturnayova, A.; Snejdarkova, M.; Hianik, T.; Spinella, K.; Mosiello, L. Development of electrochemical aptasensor using dendrimers as an immobilization platform for detection of Aflatoxin B1 in food samples. In *AISEM Annual Conference, 2015 XVIII*; IEEE, 2015; pp 1–4.
- (33) Evtugyn, G.; Porfireva, A.; Stepanova, V.; Sitdikov, R.; Stoikov, I.; Nikolelis, D.; Hianik, T. *Electroanalysis* **2014**, *26* (10), 2100–2109.
- (34) Dadmehr, M.; Shahi, S. C.; Malekkiani, M.; Korouzhdehi, B.; Tavassoli, A. *Food Chem.* **2023**, *402*, No. 134212.
- (35) Ge, G.; Wang, T.; Liu, Z.; Liu, X.; Li, T.; Chen, Y.; Fan, J.; Bukye, E.; Huang, X.; Song, L. *Talanta* **2023**, *265*, No. 124908.
- (36) Tavakoli, H.; Mohammadi, S.; Li, X.; Fu, G.; Li, X. *TrAC Trends in Analytical Chemistry* **2022**, *157*, No. 116806.
- (37) Zhou, W.; Dou, M.; Timilsina, S. S.; Xu, F.; Li, X. *Lab Chip* **2021**, *21* (14), 2658–2683.
- (38) Dou, M.; Sanjay, S. T.; Benhabib, M.; Xu, F.; Li, X. *Talanta* **2015**, *145*, 43–54.
- (39) Dou, M.; Sanjay, S. T.; Dominguez, D. C.; Liu, P.; Xu, F.; Li, X. *Biosens. Bioelectron.* **2017**, *87*, 865–873.
- (40) Sanjay, S. T.; Dou, M.; Sun, J.; Li, X. *Sci. Rep.* **2016**, *6*, No. 30474.
- (41) Sanjay, S. T.; Fu, G.; Dou, M.; Xu, F.; Liu, R.; Qi, H.; Li, X. *Analyst* **2015**, *140* (21), 7062–7081.
- (42) Zuo, P.; Li, X.; Dominguez, D. C.; Ye, B.-C. *Lab Chip* **2013**, *13* (19), 3921–3928.
- (43) Zhang, J.; Tavakoli, H.; Ma, L.; Li, X.; Han, L.; Li, X. *Adv. Drug Delivery Rev.* **2022**, *187*, No. 114365.
- (44) Tavakoli, H.; Zhou, W.; Ma, L.; Perez, S.; Ibarra, A.; Xu, F.; Zhan, S.; Li, X. *TrAC Trends in Analytical Chemistry* **2019**, *117*, 13–26.
- (45) Dou, M.; Macias, N.; Shen, F.; Dien Bard, J.; Domínguez, D. C.; Li, X. *EClinicalMedicine* **2019**, *8*, 72–77.
- (46) Dou, M.; Sanchez, J.; Tavakoli, H.; Gonzalez, J. E.; Sun, J.; Dien Bard, J.; Li, X. *Anal. Chim. Acta* **2019**, *1065*, 71–78.
- (47) Zhou, W.; Fu, G.; Li, X. *Anal. Chem.* **2021**, *93* (21), 7754–7762.
- (48) Ma, L.; Abugalyon, Y.; Li, X. *Anal. Bioanal. Chem.* **2021**, *413* (18), 4655–4663.
- (49) Tavakoli, H.; Hirth, E.; Luo, M.; Sharma Timilsina, S.; Dou, M.; Dominguez, D. C.; Li, X. *Lab Chip* **2022**, *22* (23), 4693–4704.
- (50) Tavakoli, H.; Zhou, W.; Ma, L.; Guo, Q.; Li, X. Paper and Paper Hybrid Microfluidic Devices for Point-of-care Detection of Infectious Diseases. In *Nanotechnology and Microfluidics*; Wiley, 2020; pp 177–209.
- (51) Zhou, W.; Sun, J.; Li, X. *Anal. Chem.* **2020**, *92* (21), 14830–14837.
- (52) Dou, M.; García, J. M.; Zhan, S.; Li, X. *Chem. Commun.* **2016**, *52*, 3470–3473.
- (53) Dou, M.; Sanjay, S. T.; Dominguez, D. C.; Zhan, S.; Li, X. *Chem. Commun.* **2017**, *53* (79), 10886–10889.

- (54) Du, W.; Li, L.; Nichols, K. P.; Ismagilov, R. F. *Lab Chip* **2009**, *9* (16), 2286–2292.
- (55) Wei, X.; Zhou, W.; Sanjay, S. T.; Zhang, J.; Jin, Q.; Xu, F.; Dominguez, D. C.; Li, X. *Anal. Chem.* **2018**, *90* (16), 9888–9896.
- (56) Fu, G.; Zhou, W.; Li, X. *Lab Chip* **2020**, *20* (12), 2218–2227.
- (57) Sanjay, S. T.; Kannan, S.; Li, X. *Advanced Sensor and Energy Materials* **2025**, *4*, No. 100142.
- (58) Thorsen, T.; Maerkl, S. J.; Quake, S. R. *Science* **2002**, *298* (5593), 580–584.
- (59) Jin, Q.; Ma, L.; Zhou, W.; Shen, Y.; Fernandez-Delgado, O.; Li, X. *Chemical Science* **2020**, *11* (11), 2915–2925.
- (60) Ma, X.; Wang, W.; Chen, X.; Xia, Y.; Duan, N.; Wu, S.; Wang, Z. *Food Control* **2015**, *47*, 545–551.
- (61) Martinez, A. W. *Bioanalysis* **2011**, *3* (23), 2589–2592.
- (62) Dou, M.; Dominguez, D. C.; Li, X.; Sanchez, J.; Scott, G. *Anal. Chem.* **2014**, *86* (15), 7978–7986.
- (63) Wong, S. Y.; Cabodi, M.; Rolland, J.; Klapperich, C. M. *Anal. Chem.* **2014**, *86* (24), 11981–11985.
- (64) Martinez, A. W.; Phillips, S. T.; Carrilho, E.; Whitesides, G. M. *Anal. Chem.* **2010**, *82*, 3–10.
- (65) Hu, K.; Ma, L.; Wang, Z.; Fernandez-Delgado, O.; Garay, Y. E.; Lopez, J. A.; Li, X. *ACS Sustainable Chem. Eng.* **2022**, *10* (32), 10579–10589.
- (66) Cai, Y.; Guo, G.; Fu, Y.; Huang, X.; Wang, T.; Li, T. *Chinese Journal of Analytical Chemistry* **2024**, *52* (6), No. 100408.
- (67) Liu, X.; Aizen, R.; Freeman, R.; Yehezkeili, O.; Willner, I. *ACS Nano* **2012**, *6* (4), 3553–3563.
- (68) Liang, L.; Su, M.; Li, L.; Lan, F.; Yang, G.; Ge, S.; Yu, J.; Song, X. *Sens. Actuators, B* **2016**, *229*, 347–354.
- (69) Li, H.; Fang, X.; Cao, H.; Kong, J. *Biosens. Bioelectron.* **2016**, *80*, 79–83.
- (70) Mahoney, N.; Molyneux, R. J. *Journal of agricultural and food chemistry* **2010**, *58* (7), 4065–4070.
- (71) Li, F.; Zhao, X.; Jiao, Y.; Duan, X.; Yu, L.; Zheng, F.; Wang, X.; Wang, L.; Wang, J. S.; Zhao, X.; et al. *Environmental Science and Pollution Research* **2023**, *30* (2), 3759–3759.



CAS BIOFINDER DISCOVERY PLATFORM™

CAS BIOFINDER HELPS YOU FIND YOUR NEXT BREAKTHROUGH FASTER

Navigate pathways, targets, and
diseases with precision

Explore CAS BioFinder

